INSTITUTE OF PHYSICS PUBLISHING NONLINEARITY

Nonlinearity **20** (2007) 51–74 doi:10.1088/0951-7715/20/1/004

Wavetrain response of an excitable medium to local stochastic forcing

R E Lee DeVille and Eric Vanden-Eijnden

Courant Institute of Mathematical Sciences, New York University, New York, NY 10012, USA

E-mail: deville@cims.nyu.edu and eve2@cims.nyu.edu

Received 11 February 2006, in final form 26 October 2006
Published 1 December 2006
Online at stacks.iop.org/Non/20/51

RecommendedbyLRyzhik

Abstract

We consider the effect of stochastic forcing on a one-dimensional excitable reaction–diffusion system, where the noise only acts on a small subdomain of the medium. We show that there are distinguished scaling limits in which the stochastic forcing gives rise to a mean response of a periodic wavetrain of pulses which are deterministic in the limit. Thus, the system responds coherently and periodically to stochastic forcing. This is an instance of self-induced stochastic resonance, which has previously only been analysed for finite-dimensional systems.

Mathematics Subject Classification: 60H15, 60F10, 35R60, 35K57

1. Introduction and main results

Excitable media are spatially extended systems which, in certain situations, propagate signals without loss. Excitable media play a large role in creating various phenomena, most notably in biology. Some well-known examples include the Hodgkin–Huxley equations from neuroscience [19] and the Belousov–Zhabotinskii chemical reaction [17]. Excitable media typically share certain features: a rest state which is stable to small perturbations, a dynamical structure in which larger perturbations trigger a large excursion in phase space and a refractory regime where the system is resistant to further stimulation for some time.

It is well known that excitable media support a wide variety of structures even in one dimension; in particular, they support travelling waves. The properties of such structures have been extensively studied [7, 17, 26, 27], as has their stability [12, 20]. In particular, the evolution of complicated initial data is well understood [14, 17, 27]. In many scenarios, the system settles down to a series of travelling pulses whose boundaries can be modelled by moving interfaces [1, 14].

The question of how an excitable medium reacts to stochastic forcing has been explored to a lesser degree [23, 24]. It is known that stochastic forcing of media can lead to nucleation of

pulses ([6,13], also [16] and the references therein), but typically there is significant randomness in the system due to the randomness in the forcing.

On the other hand, it is also known that, in finite-dimensional systems at least, coherence in stochastically forced dynamical systems can be generated by careful matching of timescales. This phenomenon has been termed as *self-induced stochastic resonance* (SISR) [2, 3, 10]. It was speculated in [4] that SISR may arise in infinite-dimensional systems, and further evidence of this claim was obtained via numerical simulations in [18].

This paper establishes the existence of SISR in an example of an infinite-dimensional excitable system. In particular, we show that stochastic forcing can generate periodic travelling wavetrains in the following stochastically forced reaction–diffusion equation

$$\begin{aligned} \epsilon \frac{\partial u}{\partial t} &= \epsilon^2 \frac{\partial^2 u}{\partial x^2} + f(u, v) + \delta\epsilon\eta(x, t), \\ \frac{\partial v}{\partial t} &= \epsilon^2 \frac{\partial^2 v}{\partial x^2} + g(u, v), \end{aligned} \tag{1}$$

with $x \in \mathbb{R}$, $t > 0$ and $\epsilon, \delta > 0$. The boundary conditions and the reaction terms f and g are specified in section 1.1, and $\eta(x, t)$ is a random forcing term which is specified in section 1.2. For now, it suffices to say that the reaction terms are chosen so that the medium sustains travelling waves, and the stochastic forcing is such that it acts in a small neighbourhood of one particular point.

At random times, the noise will cause pulses to nucleate near this particular point. These pulses lead to travelling waves in the medium. If the parameters are chosen properly, these travelling waves will move outwards and away from the point of generation. Since the forcing is random, we expect that, in general, the generated wavetrain itself will be random.

Here we show that there are cases where these wavetrains are coherent in space and time. Clearly this may only happen if δ is small, but if we simply let $\delta \to 0$ with ϵ fixed, it can be shown that pulses will be generated with Poisson statistics and the mean time between pulses will be $O(\exp(C\delta^{-2}))$ for some C. In particular, no pulses will appear on any finite time domain in the limit with $\delta \to 0$ and ϵ fixed. However, in section 1.2, we show that if we consider the distinguished limit

$$\delta \to 0, \qquad \epsilon \to 0, \qquad \delta^2 \log \epsilon^{-1} \to \beta, \tag{2}$$

then the times at which pulses (and anti-pulses) are created become deterministic and $O(1)$. Using formal asymptotic analysis, we will reduce the stochastic partial differential equation (SPDE) defined in (1) to a front-propagation model using delay equations with boundary conditions determined by the stochastic forcing. We then study this front-propagation model rigorously. At the level of the front-propagation model, the stochastic forcing at the origin gives rise to a periodic generation of pulses. Thus, the scaling limit that we consider in this paper is equivalent, at the level of the front-propagation model at least, to the case where we force the equation with a periodic Dirichlet boundary condition.

The analysis below shows that for an open set of choices of β in (2), the solution of the front-propagation model settles down to a space-time periodic sequence of pulses moving through the medium. To state the main results of this paper with more precision, we need to develop some preliminary material. In section 1.1 we describe the relevant dynamics of the deterministic partial differential equation (PDE), i.e. where we set $\delta = 0$ in (1). In section 1.2 we describe the effect of noise on pulse nucleations and motivate the distinguished limit we consider in this paper. Finally, in section 1.3 we state the main results of the paper.

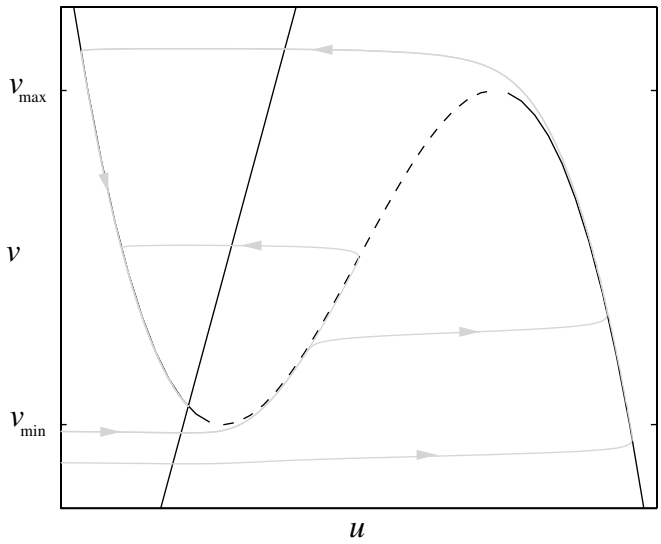

Figure 1. The u-nullcline (the set where $f(u, v) = 0$) is the cubic curve and the v-nullcline (the set where $g(u, v) = 0$) is the straight line. The middle branch of the u-nullcline is drawn dotted to stress that it is unstable. Some sample trajectories of the ODE (5) are drawn in grey.

1.1. Deterministic PDE dynamics

If we set $\delta = 0$ in (1) we obtain

$$\begin{aligned} \epsilon \frac{\partial u}{\partial t} &= \epsilon^2 \frac{\partial^2 u}{\partial x^2} + f(u, v), \\ \frac{\partial v}{\partial t} &= \epsilon^2 \frac{\partial^2 v}{\partial x^2} + g(u, v). \end{aligned} \tag{3}$$

Here we choose f and g to be smooth functions such that their roots behave like the black curves in figure 1 (the cubic curve corresponds to f, the line to g). Specifically, we make the assumption that there is a range of $v \in [v_{\min}, v_{\max}]$ such that f has three roots, which we denote $u_-(v), u_r(v), u_+(v)$, and g is chosen so that the v-nullcline intersects the u-nullcline exactly once, on the left stable branch. We also assume that $f > 0$ (respectively, $f < 0$) for points below (respectively, above) the cubic curve and that $g > 0$ (respectively, $g < 0$) for points to the right (respectively, left) of the vertical line.

There is one point where $f(u, v) = g(u, v) = 0$, which we denote as $(u_{\mathrm{fp}}, v_{\mathrm{fp}})$. The boundary conditions we impose on (3) are

$$(u(x, t), v(x, t)) \to (u_{\mathrm{fp}}, v_{\mathrm{fp}}) \qquad \text{as } x \to \pm\infty.$$

This system is a prototypical example of an excitable medium [14]. One well-known example of (3) is the Fitzhugh–Nagumo model for electrical conduction in a neuron, where f and g can be chosen [8] as

$$\begin{aligned} f(u, v) &= u - \frac{u^3}{3} - v, \\ g(u, v) &= v + a, \qquad 1 < a < 2. \end{aligned} \tag{4}$$

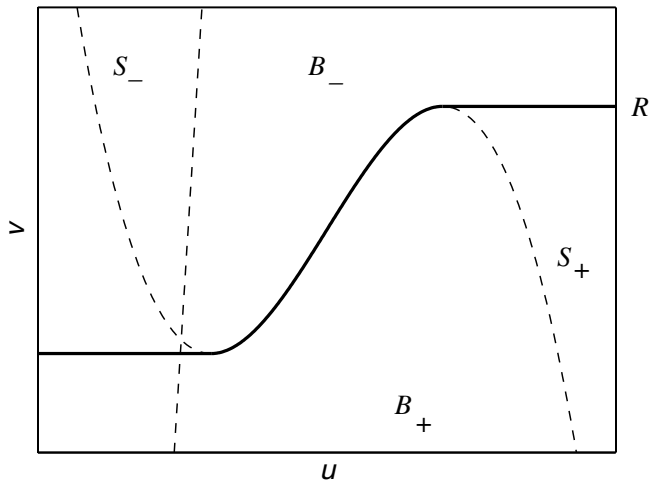

Figure 2. The nullclines are drawn as dashed lines and the separatrix R as a solid line. The region above the separatrix is S_+ and that below is S_-.

To understand the dynamics of (3), let us first consider the corresponding ODE, namely

$$\begin{aligned} \frac{\mathrm{d}u}{\mathrm{d}t} &= \frac{1}{\epsilon} f(u, v), \\ \frac{\mathrm{d}v}{\mathrm{d}t} &= g(u, v). \end{aligned} \tag{5}$$

The assumptions on the signs of f and g above imply that $(u_{\mathrm{fp}}, v_{\mathrm{fp}})$ is an attracting fixed point for (5). In figure 2, there are two sets B_+ and B_- which, in the limit $\epsilon \to 0$, are basins of attraction for (5) of the slow manifolds S_+ and S_-, respectively. By this we mean that any solution of (5) starting at a point in B_+ or B_-, for ϵ sufficiently small, first moves quickly into a neighbourhood of S_+ or S_-, respectively. If we define R to be the separatrix between B_+ and B_-, then

$$\overline{B_+} \cup \overline{B_-} = \mathbb{R}^2, \qquad \overline{B_+} \cap \overline{B_-} = R.$$

Any point which starts in B_- moves quickly to S_- and then follows S_- to the fixed point. Any point which starts in B_+ moves quickly to S_+ and moves slowly along it with increasing v. Once the point reaches the right knee at $(u_+(v_{\max}), v_{\max})$, it falls quickly onto S_- and then moves to the fixed point at $(u_{\mathrm{fp}}, v_{\mathrm{fp}})$.

In the spatially extended case (3), the situation is more complicated. For each x, if the point $(u(x,t), v(x,t))$ lies in one of $B_\pm$, then it would tend to move to one of $S_\pm$ under the reaction term in the PDE. However, if we choose initial data whose graph crosses the separatrix, then the reaction term gives rise to an interface in the solution. For example, consider initial data where at some point $\tilde{x}$, $(u_0(\tilde{x}), v_0(\tilde{x})) \in R$, but

$$(u_0(x), v_0(x)) \in \begin{cases} B_- & x < \tilde{x}, \\ B_+, & x > \tilde{x}. \end{cases}$$

Then, for $x < \tilde{x}$ (respectively, $x > \tilde{x}$), the reaction term pushes $u(x,t)$ towards S_- (respectively, S_+). In the absence of diffusion, this would lead to a discontinuity in the solution, but the diffusion term regularizes things and gives rise to smooth interfaces which become sharper as $\epsilon \to 0$.

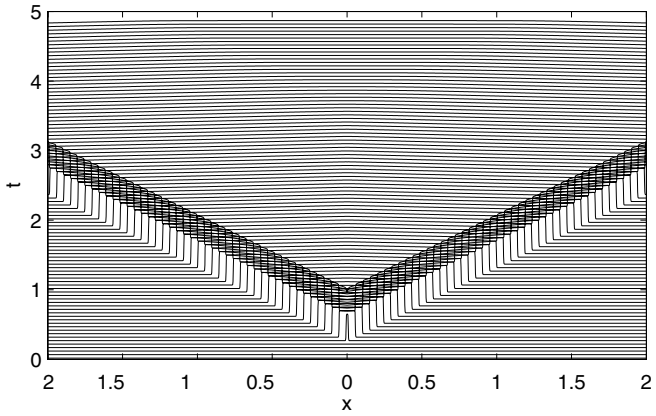

Figure 3. The long-term dynamics of a single pulse. This is a solution of (3) using (4) for the reaction term, where a single pulse has been injected.

The sense in which this medium is excitable is as follows: just as the ODE system has a unique fixed point $(u_{\mathrm{fp}}, v_{\mathrm{fp}})$, the PDE system has the spatially homogeneous fixed point

$$(u(x), v(x)) \equiv (u_{\mathrm{fp}}, v_{\mathrm{fp}}).$$

If we perturb this solution slightly, it will relax back to this fixed point. However, if we give it a large enough perturbation, it undergoes a complicated motion. For example, if we add a pulse of sufficient energy to the system, it was shown in [14] that for typical choices of f and g, the system undergoes the complicated dynamical sequence pictured in figure 3. Two wavefronts form at the edges of this pulse and subsequently move outwards. Eventually, points inside this excited region will fall off S_+ onto S_-, and so an anti-pulse forms, creating two wavebacks which also move outwards. There are then two pulses moving outwards, each with a wavefront and a waveback, and they settle down to a certain distinguished speed (which we denote by c_0) and continue to move outwards at this constant rate. The analysis in [14] models the shocks by delay equations and shows that the picture described is robust with respect to perturbations in this model. In several contexts, these pulses have been shown to be stable with respect to perturbations in the PDE as well (for example, see [1, 12, 25]).

There is one wavespeed c_0 because the medium in front of the pulse relaxes to the state $(u_{\mathrm{fp}}, v_{\mathrm{fp}})$ and the pulse moves through a medium which is completely relaxed. As we discuss below, the speed of a pulse depends on the values of $(u(x, t), v(x, t))$ at the wavefront. Since the medium is in the relaxed state in front of a pulse, there is a wavespeed corresponding to this relaxed state which gives us the speed of a pulse. Since there is only one fixed point in the dynamics of (5) (and it is attracting), there is only one speed at which a single pulse will move.

In this paper we consider a case where many pulses are injected at the same point as in figure 4. We will inject these pulses rapidly enough so that the medium does not have time to relax before the arrival of the next pulse. This allows the pulses to move at a speed different from c_0, and what we will obtain in this case is a spatially periodic profile of pulses moving at a constant speed different from c_0. The analysis in this paper is analogous to that in [14], in that we only show our solutions are robust to perturbations in the front-propagation model. We do not show that the solutions that we describe are stable with respect to perturbations of the PDE.

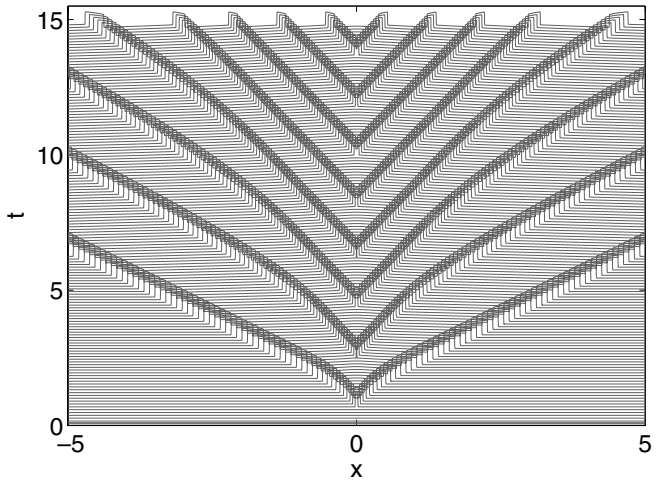

Figure 4. The evolution of many pulses. Note that the wavespeed differs between the initial pulse and the later pulses. In this simulation, the pulses were applied for $t = 0.3$ time units, while the refractory period was $t = 1.5$ time units. Here f and g are chosen as in (4).

1.2. Stochastic forcing

We now consider the full SPDE with $\delta > 0$, where we recall (1)

$$\epsilon \frac{\partial u}{\partial t} = \epsilon^2 \frac{\partial^2 u}{\partial x^2} + f(u, v) + \delta\epsilon\eta(x, t),$$

$$\frac{\partial v}{\partial t} = \epsilon^2 \frac{\partial^2 v}{\partial x^2} + g(u, v),$$

where f and g are as in the previous section, $0 < \delta, \epsilon \ll 1$ and $\eta(x, t)$ is chosen to be a stochastic process acting in a small neighbourhood of the origin: specifically, we choose $\eta(x, t) = \chi_{[-\sqrt{\epsilon},\sqrt{\epsilon}]}(x)\partial^2 W(x, t)/\partial t \partial x$ where $W(x, t)$ is the Wiener process. Thus, $\eta(x, t)$ is a white-noise process which is delta-correlated in both space and time, but only acts on a $\sqrt{\epsilon}$-size neighbourhood of the origin. (We are choosing $\sqrt{\epsilon}$ here only for concreteness; in fact, any function $\phi(\epsilon)$ with $\epsilon \ll \phi(\epsilon) \ll 1$ would do.) It was shown, e.g. in [9] that (1) makes sense even with such rough forcing.

Let us first assume that the system is unexcited at the origin, so that $u(0) = u_-(v_0)$, $v(0) = v_0$. We rescale (1) by choosing $\tau = t/\epsilon, \xi = x/\epsilon$, giving

$$\begin{aligned} \frac{\partial u}{\partial \tau} &= \frac{\partial^2 u}{\partial \xi^2} + f(u, v) + \delta\eta(x, t), \\ \frac{\partial v}{\partial \tau} &= \epsilon \left(\frac{\partial^2 v}{\partial \xi^2} + g(u, v) \right), \end{aligned} \tag{6}$$

with $v(\xi, 0) \equiv v_0$ and $u(\xi, 0) = u_-(v_0)$. Notice that in these variables, the forcing now takes place on an $\epsilon^{-1/2}$-size neighbourhood of the origin.

Since v is smooth in the original x variable, it must be nearly constant in the ξ variable, i.e. the derivative of v with respect to ξ must be $O(\epsilon)$. Because of this we will replace $v(\xi, \tau)$ with $v(\tau)$ in what follows.

We now pose the question: how long would we have to wait until the system (6) nucleates a pulse? Denoting

$$a(\delta) \asymp b(\delta) \qquad \text{if} \quad \frac{\log a(\delta)}{\log b(\delta)} \to 1 \quad \text{as } \delta \to 0,$$

it is a standard result of large-deviation theory [5, 6, 11, 15, 21] that the timescale of switching between the unexcited and excited states scales as

$$\tau^{\delta}(v) \asymp \exp(\delta^{-2}\Delta E_{+}(v)),$$

where (this is derived in [21]) $\Delta E_{+}(v)$ is the activation energy of the saddle point. To compute this energy, we define the saddle point as the solution to

$$\frac{\partial^2 u}{\partial x^2} + f(u, v) = 0, \qquad u(\pm\infty) = u_{-}(v). \tag{7}$$

We then define

$$\Delta E_{+}(v) = \int_{-\infty}^{\infty} (u_x^2 - 2F(u, v) + 2F(u_{-}(v), v))\,\mathrm{d}x, \tag{8}$$

where F is any anti-derivative of f, namely

$$F(u, v) = \int^{u} f(s, v)\,\mathrm{d}s. \tag{9}$$

We can compute many properties of (8), but it suffices for our exposition here to note that $\Delta E_{+}(v)$ is $O(1)$ in δ and ϵ, and further it is monotone increasing in v. To see why this should be so, convert the equation for the saddle point to the system

$$\frac{\mathrm{d}y}{\mathrm{d}x} = z, \qquad \frac{\mathrm{d}z}{\mathrm{d}x} = f(y, v)$$

and see that the solution to (7) corresponds to motion in an inverted potential and the saddle point solution corresponds to a homoclinic orbit starting and ending at $(u_{-}(y), 0)$. A straightforward phase-plane analysis shows that as we increase v, the size of the heteroclinic orbit decreases monotonically. This suggests that $\partial_v \Delta E_{+}(v) < 0$; for a proof that $\Delta E_{+}(v)$ is monotone decreasing, see sections 11.5 and 12.4 of [19].

Now, let us consider (1) in the limit where

$$\delta^2 \log \frac{1}{\epsilon} \to \beta, \tag{10}$$

with β being some $O(1)$ real number. If we now choose v_n so that $\Delta E_{+}(v_n) = \beta$, then it is easy to see that

$$\begin{cases} \tau^{\delta}(v) \ll \epsilon^{-1}, & \text{if } v < v_n, \\ \tau^{\delta}(v) \gg \epsilon^{-1}, & \text{if } v > v_n. \end{cases}$$

In particular, if $v < v_n$, then a pulse will nucleate with probability one on a timescale of ϵ^{-1}. Similarly, if $v > v_n$, then with probability one no pulse will nucleate on that timescale.

We can also see in this scaling that $v_\tau = O(\epsilon)$, so that v changes slowly. In particular, if we let this scaled SPDE evolve for time much less than ϵ^{-1}, very little will happen to v.

If $v > v_n$, then on a $O(\epsilon^{-1})$ timescale in τ, nothing interesting happens: v will change slowly (and change by an $O(1)$ amount in this time), but $u(x, t)$ stays close to $u_{-}(v)$. Since the dynamics of v are governed by

$$\frac{\mathrm{d}v}{\mathrm{d}t} = \epsilon g(u_{-}(v), v) =: \epsilon G_{-}(v) < 0, \tag{11}$$

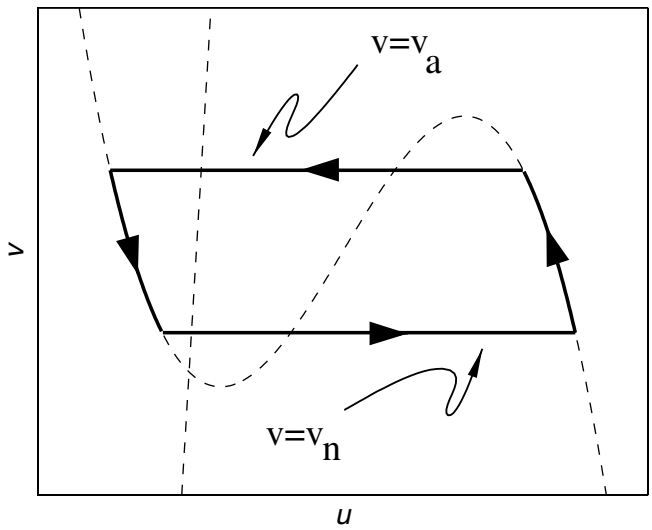

Figure 5. Graph of effective forcing in the (u, v)-plane. The system moves along S_+ and jumps left at $v = v_a$, then moves along S_- and jumps right at $v = v_n$ and repeats.

v will slowly decrease during this time. This remains true until $v \leqslant v_n$. Now, the nucleation time becomes much less than ϵ^{-1}, so that before v can change by any $O(1)$ amount a pulse will be nucleated.

In short, in the limit considered in (10), whenever the system reaches v_n at the origin and is unexcited, a pulse will nucleate in a small neighbourhood of the origin.

We can similarly define an anti-nucleation action as in (7), (8). By a similar argument, if the system is excited near the origin, but $v \geqslant v_a$, where $\Delta E_-(v_a) = \beta$, then an anti-pulse will be created in a small neighbourhood of the origin. As before, if $v < v_a$, then the anti-pulse takes much longer than ϵ^{-1} to nucleate, and v can change by an $O(1)$ amount before an anti-nucleation occurs. Thus the dynamics of v are governed by

$$\frac{\mathrm{d}v}{\mathrm{d}t} = \epsilon g(u_+(v), v) =: \epsilon G_+(v) > 0. \tag{12}$$

Summarizing. In taking the distinguished limit (10) and letting v_n, v_a solve

$$\Delta E_+(v_n) = \Delta E_-(v_a) = \beta,$$

we obtain a forcing which is pictured in figure 5. The mathematical description is as follows: choose $v_n, v_a \in [v_{\min}, v_{\max}]$ with $v_n < v_a$ and define $G_\pm(v)$ as in (11), (12). Let $V_+(t)$ be the solution of

$$\frac{\mathrm{d}V_+(t)}{\mathrm{d}t} = G_+(V_+(t)), \qquad V_+(0) = v_n,$$

and define t_+ so that $V_+(t_+) = v_a$. Similarly, let $V_-(t)$ be the solution of

$$\frac{\mathrm{d}V_-(t)}{\mathrm{d}t} = G_-(V_-(t)), \qquad V_-(0) = v_a,$$

and define t_- so that $V_-(t_-) = v_n$. Then the forcing is effectively a series of periodic pulses that are excited for time t_+ and unexcited for time t_-. Thus, at the origin the system will look like the trajectory in figure 5.

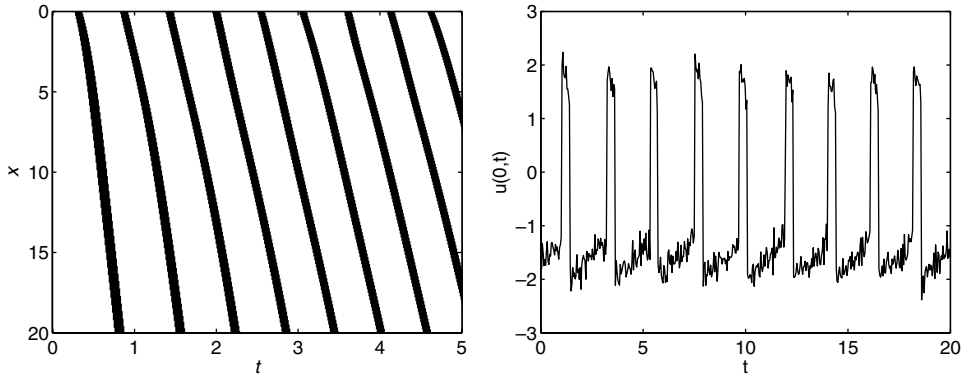

Figure 6. The solution to (1), choosing $\epsilon = 10^{-4}$ and $\delta = 20$. In the left panel, black represents where the solution is excited ($u > 1$), and white where it is not. We only show $x > 0$ in the left panel, as the solution is symmetric under the change $x \mapsto -x$. The right panel is a trace versus time of $u(0, t)$.

Figure 6 is a direct simulation of (1). We can see that pulses are being created at the origin with a high degree of regularity. The variance in the period is small since we are close to the limit in (10). The solution is even smoother away from the origin, because the randomness in the pulse creation times gets smoothed out. Away from the origin the solution looks completely periodic in space-time. The analysis contained in the rest of this paper will show that this supposition is true: if the pulses are created at the origin under the stochastic process, away from the origin the solution looks like a travelling wavetrain which is periodic in space and time.

1.3. Summary of main results

The main results of this paper combine the analyses in the previous two sections. First we derive a front-propagation model to replace the SPDE in (1). One aspect of this model is that the speed at which a shock moves through the medium is governed by the value of v at the location of the shock. We define the functions $c_{\mathrm{f}}(v)$ (respectively, $c_{\mathrm{b}}(v)$), as the speed at which a wavefront (respectively, waveback) moves through the medium, given v at the location of the shock.

As shown in section 1.2, the effect of the stochastic forcing is to introduce pulses and anti-pulses with the following properties: pulses are created when $v = v_n$ and anti-pulses are created when $v = v_a$. As we show below, each pulse leads to a pair of outward-moving wavefronts and each anti-pulse to a pair of outward-moving wavebacks. Depending on the choice of f and g in (1), it is possible that $c_{\mathrm{f}}(v_n)$ is equal to $c_{\mathrm{b}}(v_a)$ and also that they are unequal. We call the case where these are the same 'matching' wavespeeds.

When the wavespeeds match, this means that the structures being created at the origin are consistent with the deterministic propagation of waves through the medium. When each shock is created, it is created at the 'correct' wavespeed; in particular, its initial velocity matches the speed of the previous shock, and as we show below this means that the wavetrain is stable and the velocities of the fronts are constant (after transient effects are removed).

When the wavespeeds do not match, the structures being created at the origin are not consistent with the deterministic propagation; specifically, shocks are created which initially move at different speeds. Clearly, one of the two outcomes is necessary: either the velocities

of adjacent shocks relax to the same wavespeed or they eventually crash into one another. We show that the latter does not occur and that the speeds of the shocks settle down to the same constant. Moreover, we can say more: we show that once t_+, t_- are chosen by the forcing, there is exactly one wavetrain which has temporal period $t_+ + t_-$ and whose shocks move with constant velocity. We further show that the solution to the front-propagation model is a wavetrain which asymptotically approaches this particular constant-velocity wavetrain.

The rest of this paper is devoted to substantiating these claims and is organized as follows. Section 2 contains an asymptotic analysis of a series of travelling shocks in our system and derives the front-propagation model. In sections 3 and 4 we describe the long-term dynamics of these interaction equations and derive their important features—section 3 is for the case of matching wavespeeds and section 4 is for non-matching wavespeeds.

2. Derivation of travelling wave approximation

We want to develop a front-propagation model for the SPDE (1). We showed in section 1.2 that the effect of the noise is to generate a sequence of pulses at the origin, so for the rest of this paper we study the long-term dynamics of introducing these pulses into equation (3). This analysis of this section is an extension of that done in [14]; most of the contents of section 2.1 are reproduced from [14], with different notations, for completeness.

A kinematic model for the dynamics of a similar periodically forced reaction–diffusion equation was also derived in [22]. The constant-velocity solutions were characterized and, in addition, a thorough numerical study of different parameter regimes was undertaken. In particular, a much richer set of constant-velocity solutions than just periodic wavetrains was observed there (e.g. the existence of wave separations of differing lengths). The results obtained here are consistent with the numerical results observed in [22] in the monotone region of the dispersion relation (q.v. figure 1-B of [22]); moreover, we show below that the constant-velocity wavetrains observed numerically are stable and attracting in the context of the front-propagation model.

2.1. Asymptotic analysis for single shock

Let us first consider the naive expansion where we set $\epsilon = 0$ in (3); we get the outer expansion

$$\begin{aligned} 0 &= f(u, v), \\ \frac{\partial v}{\partial t} &= g(u, v). \end{aligned} \tag{13}$$

It is possible that the initial data have not been prepared so that $f(u, v) = 0$, giving rise to an initial layer. We expect this initial layer to be of size $O(\epsilon)$ in t because of the $1/\epsilon$ in the u-equation in (3). Rescaling (3) with $\tau = \epsilon t$ gives

$$\begin{aligned} \frac{\partial u}{\partial \tau} &= f(u, v), \\ \frac{\partial v}{\partial \tau} &= 0. \end{aligned} \tag{14}$$

As we can see in figure 2, almost the entire plane is the union of $B_\pm$, the basins of attraction of the manifolds $S_\pm$. For each $x \in \mathbb{R}$, the point $(u(x, 0), v(x, 0))$ lies at some point in the (u, v)-plane and will evolve according to (14). If $(u(x, 0), v(x, 0))$ is in either of $B_\pm$, it will move to the corresponding $S_\pm$ in $O(1)$ time. Moreover, if the initial data lie inside some compact set K, then every point in $B_\pm$ will move to a given small neighbourhood of $S_\pm$ in some $O(1)$ time τ_0 which can be chosen uniformly in x. Any x where the initial data lie on

the separatrix will become a discontinuity of the outer expansion (13). Moreover, since this evolution happens in an $O(1)$ time in τ, it happens in an $O(\epsilon)$ time in t.

Solving the first equation of (14) gives $u(x,t) = u_\pm(v(x,t))$, so that the medium can be in one of the two states. From this, (13) gives

$$\frac{\partial v}{\partial t} = G_\pm(v) := g(u_\pm(v), v).$$

If u is excited ($u = u_+(v)$) at the point x, then v evolves by

$$\frac{\mathrm{d}v}{\mathrm{d}t}(x,t) = G_+(v), \tag{15}$$

and similarly, if it is refractory ($u = u_-(v)$), then v evolves by

$$\frac{\mathrm{d}v}{\mathrm{d}t}(x,t) = G_-(v). \tag{16}$$

The outer expansion thus generates discontinuities in u for generic initial data. Any solution to (3) must be smooth because of the diffusion, so these discontinuities will give rise to a boundary layer of width $O(\epsilon)$ in x. Therefore, we do an inner expansion near one of these shocks. We expect these shocks to move, leading us to the travelling wave Ansatz

$$\xi = \frac{x - y(t)}{\epsilon}.$$

For concreteness, let us first consider the 'down'-shock, namely a discontinuity where

$$\lim_{x \to y(t)_-} = u_+(v(y(t),t)), \qquad \lim_{x \to y(t)_+} = u_-(v(y(t),t)).$$

In what follows, we will consider right-moving shocks, and so down-shocks will be wavefronts. Plugging the inner expansion into (3) for $U(\xi,t)$, $V(\xi,t)$ gives

$$\begin{aligned} &\frac{\partial^2 U}{\partial \xi^2} + \frac{\mathrm{d}y}{\mathrm{d}t}\frac{\partial U}{\partial \xi} + f(U,V) = 0, \\ &\frac{\mathrm{d}y}{\mathrm{d}t}\frac{\partial V}{\partial \xi} = 0, \end{aligned} \tag{17}$$

supplemented with the boundary conditions

$$U(\pm\infty) = u_\mp(v).$$

First, note that as long as $\dot{y}(t) \neq 0$, V is constant in ξ and, in fact, is the same as the value v at the shock. Moreover, since $\dot{y}$ and V do not depend on ξ, (17) is simply an ODE for U in ξ. The boundary conditions give a solvability condition for (17); it is a standard result (see section 11.5 of [19] for a boundary-value analysis) that there is a unique value $c_\mathrm{f}(v)$ for which

$$\begin{aligned} &\frac{\partial^2 U}{\partial \xi^2} + c_\mathrm{f}(v)\frac{\partial U}{\partial \xi} + f(U,v) = 0, \\ &U(\pm\infty) = u_\mp(v) \end{aligned} \tag{18}$$

has a solution (the solution is itself unique up to translation). Thus $c_\mathrm{f}(v)$—the wavespeed of the shock—depends only on the value of v at the shock. We can similarly consider an 'up'-shock, which is a point of discontinuity where

$$\lim_{x \to y(t)_-} = u_-(v), \qquad \lim_{x \to y(t)_+} = u_+(v).$$

Changing variables from $\xi \mapsto -\xi$ in (17) shows that if we consider the down-shock and the up-shock with a given value of v, these two shocks have opposite wavespeeds. We denote

$$c_\mathrm{b}(v) = -c_\mathrm{f}(v)$$

to be the wavespeed of an up-shock (waveback for a right-moving wave). If we define F as in (9), then we can solve for $c_{\mathrm{f}}(v)$ in (17) to get

$$c_{\mathrm{f}}(v) = -\frac{[F]_v}{\|u'(\xi)\|_{L^2}^2}, \tag{19}$$

where $[F]_v$ is the potential jump

$$[F]_v = F(u_+(v), v) - F(u_-(v), v) = \int_{u_-(v)}^{u_+(v)} f(s, v)\,\mathrm{d}s.$$

The meaning of (19) is as follows: consider a thin pulse with a local value v where $F_v(u_+(v)) < F_v(u_-(v))$. The potential well of F_v near the excited manifold is of lower energy, so we expect the excited region will grow. In fact, (19) then gives that $c_{\mathrm{f}}(v) > 0$ (and $c_{\mathrm{b}}(v) < 0$), so that the edges of the pulse will move outwards.

We will assume throughout this paper that f and g are chosen in (1) so that the function $c_{\mathrm{f}}(v)$ is a monotone decreasing function of v, that $c_{\mathrm{f}}(v_{\min}) > 0$ and $c_{\mathrm{f}}(v_{\max}) < 0$. (This is true if, for example, we choose f and g as in (4).) We will denote by $v_\star$ the unique value of v where $c_{\mathrm{f}}(v_\star) = 0$. We will also use the tilde to denote the complementary wavespeed, so $\tilde{v}$ is defined to be the solution to

$$c_{\mathrm{f}}(\tilde{v}) = c_{\mathrm{b}}(v) = -c_{\mathrm{f}}(v).$$

In particular, if we choose f and g as in (4), it is easy to see from symmetry considerations that $\tilde{v} = -v$.

2.2. *Interaction of several shocks*

What we have shown so far is that any initial data quickly evolve to a solution which has sharp transitions of width $O(\epsilon)$, and then these shocks move at $O(1)$ velocities. In the absence of forcing in the equation, this explains all the dynamics, as described in [14]. However, this analysis does not take the boundary conditions into account. As we saw in section 1.2, we have chosen a particular forcing which will, in many cases, create a series of wavefronts and wavebacks.

We want to consider only the case where all shocks move outwards from the origin or move to the right for $x > 0$. (Recall that we have chosen everything symmetrically so that we need to only study $x > 0$.) It is not clear from the outset what assumptions are necessary in the forcing so that all shocks move to the right; this is part of the analysis below.

From (18), the speed of the shock depends on the value of v at the shock. Moreover, by (15) and (16) the value of v at the shock depends on the value of v at the previous shock, as it will have evolved after the previous shock passed.

We want to write down a set of delay equations which model the evolution of these shocks. Here we track the local v-value at each shock and the temporal separation between any two adjacent shocks. The model we will develop will describe the evolution of these quantities and will finally be given in (26) and (27).

We will use the following notation: the position of the kth wavefront will be given by $x_k^{\mathrm{f}}(t)$, and the kth waveback will be given by $x_k^{\mathrm{b}}(t)$. We define t_k^{cf} to be the time of creation of the kth wavefront and t_k^{cb} the time of creation of the kth waveback. The conclusion of section 1.2 is that

$$t_k^{\mathrm{cf}} = k(t_+ + t_-), \qquad t_k^{\mathrm{cb}} = t_+ + t_k^{\mathrm{cf}}.$$

Thus $x_k^{\mathsf{f}}(t)$ is defined on some subset of $[t_k^{\mathsf{cf}}, \infty)$ and $x_k^{\mathsf{b}}(t)$ is defined on some subset of $[t_k^{\mathsf{cb}}, \infty)$. We will refer to the collection $\{x_k^{\mathsf{f}}(t), x_k^{\mathsf{b}}x(t)\}$ as $\mathcal{X}^{\mathsf{f},\mathsf{b}}(t)$ when necessary. The value of v at any of these fronts is denoted as

$$\begin{aligned} v_k^{\mathsf{f}}(t) &= v(x_k^{\mathsf{f}}(t), t), \\ v_k^{\mathsf{b}}(t) &= v(x_k^{\mathsf{b}}(t), t). \end{aligned} \tag{20}$$

We know that a shock will move with velocity determined by the local value of v, namely that

$$\dot{x}_k^{\mathsf{f}}(t) = c_{\mathsf{f}}(v_k^{\mathsf{f}}(t)), \qquad \dot{x}_k^{\mathsf{b}}(t) = c_{\mathsf{b}}(v_k^{\mathsf{b}}(t)). \tag{21}$$

(Recall that $c_{\mathsf{b}}(v) = -c_{\mathsf{f}}(v)$, although we will use both c_{f} and c_{b} for clarity.) We further want to model the temporal separation between two shocks. To this end, we define $\tau_k^{\mathsf{f}}(t)$ and $\tau_k^{\mathsf{b}}(t)$ as follows: $\tau_k^{\mathsf{f}}(t)$ is defined to satisfy

$$x_k^{\mathsf{f}}(t - \tau_k^{\mathsf{f}}(t)) = x_k^{\mathsf{b}}(t) \tag{22}$$

and $\tau_k^{\mathsf{b}}(t)$ is defined so that

$$x_k^{\mathsf{b}}(t - \tau_k^{\mathsf{b}}(t)) = x_{k+1}^{\mathsf{f}}(t). \tag{23}$$

The meaning of $\tau_k^{\mathsf{f}}(t)$ is as follows. Choose $t > t_k^{\mathsf{cb}}$ and assume that $x_k^{\mathsf{b}}(t)$ is defined and equal to some $x > 0$. Assume further that the kth wavefront existed long enough to pass x and did so at some earlier time s. Then $\tau_k^{\mathsf{f}}(t)$ is defined to be $t - s$; in words, it is how long ago the kth wavefront passed the point at which the kth waveback is at right now. This will be well defined as long as all shocks continue to exist and are unidirectional.

We define the time-t Poincare map of $G_{\pm}$ as follows: for any v_0, t, $\phi_{\pm}^t(v_0)$ is defined to be $v(t)$, where $v(t)$ solves $\dot{v} = G_{\pm}(v)$ with initial condition $v(0) = v_0$.

Recall that $c_{\mathsf{f}}(v)$ is monotone decreasing by assumption. Then it is clear that $c_{\mathsf{f}}(v_{\min})$ is the fastest possible wavefront speed and $c_{\mathsf{b}}(v_{\max})$ is the fastest possible waveback speed. However, because of the fixed point at $(u_{\mathsf{fp}}, v_{\mathsf{fp}})$, the fastest wavefront speed we want to consider will be that with $c_{\mathsf{f}}(v_{\mathsf{fp}})$, and thus

$$c_{\max} = \min(c_{\mathsf{f}}(v_{\mathsf{fp}}), c_{\mathsf{b}}(v_{\max}))$$

is the wavespeed of the fastest pulse we consider. (We need to make this restriction because otherwise there would be no way to connect the wavefront to the waveback using (16).) Now define

$$\hat{v}_{\min} = c_{\mathsf{f}}^{-1}(c_{\max}), \qquad \hat{v}_{\max} = c_{\mathsf{b}}^{-1}(c_{\max}).$$

It follows that either $\hat{v}_{\min} = v_{\mathsf{fp}}$ or $\hat{v}_{\max} = v_{\max}$ (or possibly both). In what follows, we will be considering $v \in [\hat{v}_{\min}, \hat{v}_{\max}]$, the values of v which can support travelling pulses. For $v \in [\hat{v}_{\min}, \hat{v}_{\max}]$, there is a complimentary $\tilde{v}$ which solves

$$c_{\mathsf{f}}(\tilde{v}) = -c_{\mathsf{f}}(v) = c_{\mathsf{b}}(v).$$

Say that we pick a $v \in [\hat{v}_{\min}, v_\star]$ so that $c_{\mathsf{f}}(v) > 0$. Then $\tilde{v} > v$, and we can define $\tau_+(v)$ to be the solution to

$$\phi_+^{\tau_+(v)}(v) = \tilde{v}. \tag{24}$$

We also define $\tau_-(v)$ similarly, namely

$$\phi_-^{\tau_-(v)}(v) = \tilde{v}. \tag{25}$$

Note that $\tau_+(v)$ is also a monotone decreasing function of v, and $\tau_+(v_\star) = \tau_-(v_\star) = 0$.

To compute the evolution equation for $\tau_k^{\mathsf{f}}(t)$, we differentiate (22) to obtain

$$(1 - \dot{\tau}_k^{\mathsf{f}}(t)) = \frac{\dot{x}_k^{\mathsf{b}}(t)}{\dot{x}_k^{\mathsf{f}}(t - \tau_k^{\mathsf{f}}(t))}.$$

Using (21) and solving for $\dot{\tau}_k^{\mathsf{f}}(t)$ gives

$$\dot{\tau}_k^{\mathsf{f}}(t) = 1 + \frac{c_{\mathsf{f}}(v_k^{\mathsf{b}}(t))}{c_{\mathsf{f}}(v_k^{\mathsf{f}}(t - \tau_k^{\mathsf{f}}(t)))}.$$

This equation now gives $\dot{\tau}_k^{\mathsf{f}}(t)$ in terms of v_k^{b} and v_k^{f}. But notice that

$$v_k^{\mathsf{b}}(t) = \phi_+^{\tau_k^{\mathsf{f}}(t)}(v_k^{\mathsf{f}} x(t - \tau_k^{\mathsf{f}}(t))),$$

since v evolves under (15) in the excited regime, thus

$$\dot{\tau}_k^{\mathsf{f}}(t) = 1 + \frac{c_{\mathsf{f}}(\phi_+^{\tau_k^{\mathsf{f}}(t)}(v_k^{\mathsf{f}}(t - \tau_k^{\mathsf{f}}(t))))}{c_{\mathsf{f}}(v_k^{\mathsf{f}}(t - \tau_k^{\mathsf{f}}(t)))}. \tag{26}$$

In a similar fashion, we obtain the equation

$$\dot{\tau}_k^{\mathsf{b}}(t) = 1 + \frac{c_{\mathsf{b}}(\phi_-^{\tau_k^{\mathsf{b}}(t)}(v_k^{\mathsf{b}}(t - \tau_k^{\mathsf{b}}(t))))}{c_{\mathsf{b}}(v_k^{\mathsf{b}}(t - \tau_k^{\mathsf{b}}(t)))}. \tag{27}$$

The model now has the following structure: given $v_k^{\mathsf{f}}(t)$ for all $t > t_k^{\mathsf{cf}}$, $v_k^{\mathsf{b}}(t)$ is uniquely determined. Similarly, given $v_k^{\mathsf{b}}(t)$ for all $t > t_k^{\mathsf{cb}}$, the model uniquely determines $v_{k+1}^{\mathsf{f}}(t)$. The only information we need to evolve these equations is $v_1^{\mathsf{f}}(t)$ for all $t > t_1^{\mathsf{cf}}$, which will be given by the initial data for the PDE, and t_k^{cf}, t_k^{cb} for all k, which is given by the boundary condition. The solutions $v_k^{\mathsf{f}}(t)$ for $k > 1$ and $v_k^{\mathsf{b}}(t)$ for $k \geqslant 1$ can then be uniquely generated by choosing the initial and boundary data. Once $v_k^{\mathsf{f}}(t)$ and $v_k^{\mathsf{b}}(t)$ are determined for all k, we can solve for $x_k^{\mathsf{f}}(t)$ and $x_k^{\mathsf{b}}(t)$ using (21) and the initial conditions

$$x_k^{\mathsf{f}}(t_v^{\mathsf{cf}}) = x_k^{\mathsf{b}}(t_k^{\mathsf{cb}}) = 0.$$

Determining the solutions to (26) and (27) determines the entire collection $\mathcal{X}^{\mathsf{f},\mathsf{b}}(t)$.

Moreover, although (26), (27) are, as stated, delay equations with a variable delay, it is convenient to understand them as recursively defined nonautonomous ODE. For example, consider (26) and assume that $v_k^{\mathsf{f}} x(t)$ is given for all $t > t_k^{\mathsf{cf}}$. Once $v_k^{\mathsf{f}}(t)$ has been fixed, we can write the right-hand side of (26) as some function $R(t, \tau_k^{\mathsf{f}}(t))$, and solving this nonautonomous ODE determines $\tau_k^{\mathsf{f}}(t)$ and $v_k^{\mathsf{b}}(t)$ uniquely.

3. First case: matching times

In this section we consider the case where the times match a certain periodic solution. Choose $c_\star \in (0, c_{\max}]$, and then there are v_n, $v_a \in [\hat{v}_{\min}, \hat{v}_{\max}]$ so that $c_{\mathsf{f}}(v_n) = c_{\mathsf{b}}(v_a) = c_\star$, and this gives $\tau_+(v_n)$, $\tau_-(v_a)$.

For the rest of this section, we assume that v_n, v_a have been chosen in section 1.2 so that there is a $c_\star$ with

$$t_k^{\mathsf{cb}} - t_k^{\mathsf{cf}} = \tau_+(v_n), \qquad t_{k+1}^{\mathsf{cf}} - t_k^{\mathsf{cb}} = \tau_-(v_a) \tag{28}$$

and

$$c_{\mathsf{f}}(v_n) = c_{\mathsf{b}}(v_a) = c_\star. \tag{29}$$

For simplicity, we will denote

$$t_+ = \tau_+(v_n), \qquad t_- = \tau_-(v_a).$$

In this case, the times are so contrived that if we create the kth wavefront at t_k^{cf} with $v_k^{\mathsf{f}}(t_k^{\mathsf{cf}}) = v_n$, then the kth waveback is created at time $t_k^{\mathsf{cb}} = t_k^{\mathsf{cf}} + t_+$, and this means that the local value of the back when it is created is

$$\phi_+^{\tau_+(v_n)}(v_n) = v_a.$$

Thus the kth waveback will start with the velocity which matches it to the kth front. Similarly, the $(k+1)$th wavefront is created at $t^{\mathrm{cf}}_{k+1} = t^{\mathrm{cf}}_k + t_+ + t_-$. This means that the local value of v when it is created is again v_n, which means that it will move at velocity $c_\star$. We say here that the forcing is matched to the wavespeed $c_\star$.

Thus we expect that as long as the forcing matches the wavespeed $c_\star$, and if we ever generate a pulse moving with speed $c_\star$, then all future pulses will be created (and stay) at speed $c_\star$. We will show this in proposition 1. Moreover, if we choose initial data so that the first few pulses are not created with speed $c_\star$, we might hope that the effect of the initial data is transient and that the wavespeeds limit on $c_\star$. We show that this is true in theorem 1. It is a consequence of this theorem that the periodic wavetrain is stable to perturbations (in the sense of perturbations to the travelling wave model, of course).

We first state and prove proposition 1.

Proposition 1. *Fix $c_\star$ and assume that (28) and (29) are satisfied. Assume initial data are chosen so that $v^{\mathsf{f}}_1(t) = v_n$ for all $t \in [0, T]$. Then for $x \in [0, T/c_{\mathsf{f}}(v_n)]$, the solution $\mathcal{X}^{\mathsf{f},\mathsf{b}}(t)$ to the front-propagation model developed in section 2 has*

$$v^{\mathsf{f}}_k(t) = v_n, \qquad v^{\mathsf{b}}_k(t) = v_a,$$

for all t for which these functions are defined.

Proof. This follows from an analysis of the equations given in (26), (27). We are given $v^{\mathsf{f}}_1(t) = v_n$. Then we can simplify (26) to

$$\dot\tau^{\mathsf{f}}_1(t) = 1 + \frac{c_{\mathsf{f}}(\phi_+^{\tau^{\mathsf{f}}_1(t)}(v_n))}{c_{\mathsf{f}}(v_n)}.$$

But $\tau^{\mathsf{f}}_1(0) = \tau_+(v_n)$, and thus $v^{\mathsf{b}}_1(0) = v_a$. Then $\dot\tau^{\mathsf{f}}_1(t) = 0$, and therefore $\tau^{\mathsf{f}}_1(t) = \tau_+(v_n)$ and $v^{\mathsf{b}}_1(t) = v_a$ for all $t \in [0, T]$. Continuing, (27) becomes

$$\dot\tau^{\mathsf{b}}_1(t) = 1 + \frac{c_{\mathsf{b}}(\phi_-^{\tau^{\mathsf{b}}_1(t)}(v_a))}{c_{\mathsf{b}}(v_a)}.$$

Again, since $\tau^{\mathsf{b}}_1(0) = \tau_-(v_a)$, this means $v^{\mathsf{f}}_2(0) = v_n$ and $\dot\tau^{\mathsf{b}}_1(t) = 0$ for all $t \in [0, T]$. Iterating this argument gives that

$$v^{\mathsf{f}}_k(t) = v_n, \qquad v^{\mathsf{b}}_k(t) = v_a,$$

for all $t \in [0, T]$. Since all these pulses move to the right with speed $c_{\mathsf{f}}(v_n)$, this analysis also holds on the finite domain $x \in [0, T/c_{\mathsf{f}}(v_n)]$. □

To construct initial data for the PDE so that $v^{\mathsf{f}}_1 x(t) = v_n$ for all time would be to choose, for $x > 0$,

$$v_0(x) = \phi_-^{-x/c_\star}(v_n), \qquad u_0(x) = u_-(v_0(x)). \tag{30}$$

Since the first pulse moves rightwards with speed $c_\star$, if we choose any point x, $v^{\mathsf{f}}_1(t) = x$ at $t = x/c_\star$, the initial condition has been set so that at that time, $v(x, t)$ will be exactly v_n. This is what has been done in the right frame in figure 7.

A more complicated scenario is the initial data not being prepared so that $c(v^{\mathsf{f}}_1(t)) = c_\star$. As discussed above, we expect that the first pulse will be transient on any finite spatial domain and the first pulse will move arbitrarily far from the origin. In fact, we state this explicitly in theorem 1.

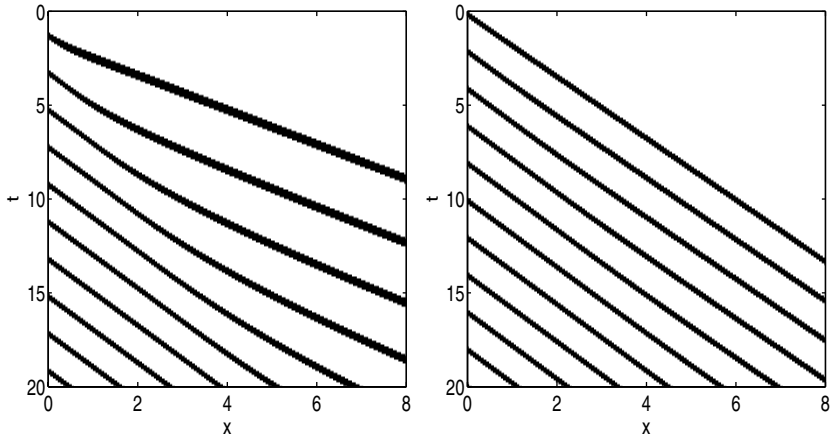

Figure 7. Simulations are of the PDE (1) with f, g chosen as in (4), with $\epsilon = 10^{-2}$, $a = 1.05$, $v_n = -0.5$, $v_a = 0.5$. In these pictures, we have plotted $u(x, t)$, and it is black when $u(x, t) > 1$, i.e. excited, and white otherwise. One can check that by symmetry $c_{\mathsf{f}}(v_n) = c_{\mathsf{b}}(v_a)$. The left frame is for the case of quiescent initial data, so that $v_1^{\mathsf{f}}(t) = v_{\mathsf{fp}}$ for all time. Here the initial data are transient, and later pulses get closer to the periodic wavetrain. The right frame is for initial data chosen (see (30)) so that $v_1^{\mathsf{f}}(t) = v_{\mathsf{fp}}$ for all t. Note that the wavetrain is space-time periodic for all time.

Theorem 1. *Assume that the forcing satisfies (28) and (29) and that the f and g in (1) are chosen so that the map $\phi_+^{t_+} \circ \phi_-^{t_-}(\cdot)$ with domain $[\hat{v}_{\min}, \hat{v}_{\max}]$ has a unique attracting fixed point. Let $v_1^{\mathsf{f}}(t) = v_0$ be constant and further assume that $\phi_+^{t_+}(v_0) > v_\star$ and $v_0 < v_\star$. Then there exists k_0 so that for $k > k_0$ the solutions $v_k^{\mathsf{f}}(t)$ (respectively, $v_k^{\mathsf{b}}(t)$) have the property that they are very close to v_n (respectively, v_a) for some finite time and then undergo a transition to a state where they match with v_0. In other words, for any $\delta > 0$, there exist $t_{k,1}, t_{k,2}$ such that*

$$\begin{cases} |v_k^{\mathsf{f}} x(t) - v_n| < \delta, & t < t_{k,1}, \\ |v_k^{\mathsf{f}}(t) - v_0| < \delta, & t > t_{k,2}, \end{cases}$$

and there exist $t_{k,3}, t_{k,4}$ such that

$$\begin{cases} |v_k^{\mathsf{b}}(t) - v_a| < \delta, & t < t_{k,3}, \\ |v_k^{\mathsf{b}} x(t) - \tilde{v_0}| < \delta, & t > t_{k,4}. \end{cases}$$

Moreover, $t_{k,i} \sim k$ as $k \to \infty$ for all i.

We delay the proof of this theorem until the end of this section, after we have proved a few lemmas. Before we state and prove these lemmas, we have a few remarks.

Remarks.

1. The fact that the map $\phi_+^{t_+}(\phi_-^{t_-}(\cdot))$ has a unique attracting fixed point means that
$$\lim_{k\to\infty} v_k^{\mathsf{f}}(t_v^{\mathsf{cf}}) \to v_n, \qquad \lim_{k\to\infty} v_k^{\mathsf{b}}(t_k^{\mathsf{cb}}) \to v_a.$$
2. If we assume that the pulses are created by the stochastic process described in section 1.2, then *a fortiori* we have
$$v_k^{\mathsf{f}}(t_k^{\mathsf{cf}}) = v_n, \qquad v_k^{\mathsf{b}}(t_k^{\mathsf{cb}}) = v_a, \qquad \text{for all } k.$$

3. The unique attracting fixed point condition is not very restrictive. Since the system (5) has an attracting fixed point at $(u_{\mathrm{fp}}, v_{\mathrm{fp}})$, as long as t_- is chosen large enough (or, equivalently, v_n is chosen close enough to v_{fp}), the composition of the Poincaré maps will be uniformly contracting.
4. Even though the theorem is stated and proved for the case where the first wavefront moves at a constant speed, this is not a real restriction to the theory. It is clear from the proof of theorem 1 that if the first wavefront moved at a variable (but bounded above and below) speed, this effect would be transient and eventually pulses would be moving at the speed $c_\star$.

Lemma 2. *Choose* $A, B \in [\hat{v}_{\min}, \hat{v}_{\max}]$, $\delta > 0$ *so that*

$$\|v_k^{\mathrm{f}}(t) - A\|_{[t_k^{\mathrm{cf}}, t_1]} < \delta,$$

$$\|v_k^{\mathrm{f}}(t) - B\|_{[t_2, \infty)} < \delta,$$

for some t_1, t_2 *and where we denote*

$$\|f(t)\|_{[a,b]} = \sup_{t\in[a,b]} (|f(t)| + |f'(t)|).$$

We further assume that

$$|\tau_k^{\mathrm{f}}(t_k^{\mathrm{cb}}) - \tau_+(A)| < \delta, \qquad |\tau_k^{\mathrm{b}}(t_{k+1}^{\mathrm{cf}}) - \tau_-(\tilde{A})| < \delta.$$

Then there exist $C_1, C_2 > 0$ *independent of* k *so that*

$$\|v_{k+1}^{\mathrm{f}}(t) - A\|_{[t_{k+1}^{\mathrm{cf}}, t_3]} \leqslant C_1\delta,$$

$$\|v_{k+1}^{\mathrm{f}}(t) - B\|_{[t_4, \infty)} \leqslant C_1\delta,$$

where

$$t_3 > t_1 + \tau_+(A) + \tau_-(\tilde{A}) + C_2,$$

$$t_4 > t_2 + \tau_+(B) + \tau_-(\tilde{B}) + C_2.$$

Proof. Let us consider the ODE for $\tau_k^{\mathrm{f}}(t)$, recalling (26):

$$\dot{\tau}_k^{\mathrm{f}}(t) = 1 + \frac{c_{\mathrm{f}}(\phi_+^{\tau_k^{\mathrm{f}}(t)}(v_k^{\mathrm{f}}(t - \tau_k^{\mathrm{f}}(t))))}{c_{\mathrm{f}}(v_k^{\mathrm{f}}(t - \tau_k^{\mathrm{f}}(t)))}.$$

We first want to determine the zeros of the function

$$R(t, \tau_k^{\mathrm{f}}) = 1 + \frac{c(\phi_+^{\tau_k^{\mathrm{f}}(t)}(v_k^{\mathrm{f}}(t - \tau_k^{\mathrm{f}}(t))))}{c(v_k^{\mathrm{f}}(t - \tau_k^{\mathrm{f}}(t)))}.$$

Given $v_k^{\mathrm{f}}(t)$, this is a fixed set of points in the (t, τ_k^{f})-plane, which we denote by $\mathcal{Z}(v_k^{\mathrm{f}})$. If $v_k^{\mathrm{f}}(t_k^{\mathrm{cf}}) = V$, then

$$R(t_k^{\mathrm{cf}} + \tau_+(V), \tau_+(V)) = 1 + \frac{c(\phi_+^{\tau_+(V)}(v_k^{\mathrm{f}}(t_k^{\mathrm{cf}})))}{c(v_k^{\mathrm{f}}(t_k^{\mathrm{cf}}))} = 1 + \frac{c(\phi_+^{\tau_+(V)}(\tau_+(V))V)}{c(V)} = 0,$$

so that $(t_k^{\mathrm{cf}} + \tau_+(V), \tau_+(V)) \in \mathcal{Z}(v_k^{\mathrm{f}})$. Considering $t > t_k^{\mathrm{cf}}$, the set $\mathcal{Z}(v_k^{\mathrm{f}})$ will contain a curve in the plane parametrized by

$$(t + \tau_+(v_k^{\mathrm{f}}(t)), \tau_+(v_k^{\mathrm{f}}(t))). \tag{31}$$

The tangent vector to this curve is given by

$$(1 + \tau_+'(v_k^{\mathrm{f}}(t))\dot{v}_k^{\mathrm{f}}(t),\, \tau_+'(v_k^{\mathrm{f}}(t))\dot{v}_k^{\mathrm{f}}(t)),$$

which we will denote more simply as

$$(1 + \alpha(t), \alpha(t)).$$

It is straightforward to calculate that

$$\frac{\mathrm{d}}{\mathrm{d}Q}\tau_+(Q) = -\left(\frac{1}{G_+(Q)} + \frac{c'(Q)}{G_+(\widetilde{Q})c'(\widetilde{Q})}\right),$$

and thus there are constants $C_1 < C_2 < 0$ with

$$C_1\dot{v}_k^{\mathrm{f}}(t) < \alpha(t) < C_2\dot{v}_k^{\mathrm{f}}(t).$$

In particular, $\alpha(t)$ and $\dot{v}_k^{\mathrm{f}}(t)$ always have opposite signs.

For $t \in [t_k^{\mathrm{cb}}, t_1 + \tau_+(A)]$, $\mathcal{Z}(v_k^{\mathrm{f}})$ contains a curve which is very close to $\tau_+(A)$; more specifically we have

$$\|\mathcal{Z}(v_k^{\mathrm{f}}) - \tau_+(A)\|_{[t_k^{\mathrm{cb}}, t_1+\tau_+(A)]} < \sqrt{2}\delta,$$

if we consider the set of points as a function of t in the (t, τ_k^{f})-plane. The same argument shows that $\mathcal{Z}(v_k^{\mathrm{f}}x)$ contains a curve almost equal to the constant $\tau_+(B)$ for $t > t_2 + \tau_+(B)$.

We have determined the set of roots $\mathcal{Z}(v_k^{\mathrm{f}})$. We will show below in lemma 3 that as long as $|\dot{v}_k^{\mathrm{f}}(t)|$ is sufficiently small, this set is attracting in the τ_k^{f} direction in the (t, τ_k^{f})-plane. It is a straightforward calculus estimate to show that there is a $C_3 > 0$ such that

$$\|\tau_k^{\mathrm{f}}(t) - \tau_+(A)\|_{[t_k^{\mathrm{cb}}, t_1+\tau_+(A)]} < C_3\delta.$$

Moreover, since the right-hand side of (26) is bounded above, there is a $C_7 > 0$ such that

$$\|\tau_k^{\mathrm{f}}(t) - \tau_+(A)\|_{[t_k^{\mathrm{cb}}, t_1+\tau_+(A)+C_7]} < C_3\delta.$$

We want to show that $v_k^{\mathrm{b}}(t)$ is close to $\tilde{A}$, but

$$v_k^{\mathrm{b}}(t) = \phi_+^{\tau_k^{\mathrm{f}}(t)}(v_k^{\mathrm{f}}(t - \tau_k^{\mathrm{f}}(t))),$$

$\tau_k^{\mathrm{f}}(t)$ is close to $\tau_+(A)$ and $v_k^{\mathrm{f}}(t)$ is close to A. Then $v_k^{\mathrm{b}}(t)$ should be close to $\phi_+^{\tau_+(A)}(A) = \tilde{A}$. More specifically, we have that there is a $C_4 > 0$ such that

$$\|v_k^{\mathrm{b}}(t) - \tilde{A}\|_{[t_k^{\mathrm{cb}}, t_1+\tau_+(A)+C_7]} = \|\phi_+^{\tau_k^{\mathrm{f}}(t)}(v_k^{\mathrm{f}}(t - \tau_k^{\mathrm{f}}(t))) - \phi_+^{\tau_+(A)}(A)\|_{[t_k^{\mathrm{cb}}, t_1+\tau_+(A)+C_7]} \leqslant C_4\delta$$

and this C_4 is proportional to the larger of $D_t\phi_+^{\tau_k^{\mathrm{f}}}(v_k^{\mathrm{f}})$, $D_v\phi_+^{\tau_k^{\mathrm{f}}}(v_k^{\mathrm{f}})$. We can apply precisely the same argument to $v_k^{\mathrm{b}}(t)$. Similarly, there is a $C_8 > 0$ so that

$$\|\tau_k^{\mathrm{f}}(t) - \tau_-(\tilde{A})\|_{[t_{k+1}^{\mathrm{cf}}, t_1+\tau_+(A)+\tau_-(\tilde{A})+C_7+C_8]} \leqslant C_5\delta,$$

and thus

$$\|v_{k+1}^{\mathrm{f}}(t) - \phi_-^{\tau_-(\tilde{A})}(\tilde{A})\|_{[t_{k+1}^{\mathrm{cf}}, t_1+\tau_+(A)+\tau_-(\tilde{A})+C_2]} \leqslant C_1\delta,$$

for some constants $C_5, C_1 > 0$, and with $C_2 = C_7 + C_8$. This proves the lemma. □

Lemma 3. *Given $v_k^{\mathrm{f}}(t)$, there exists a function $b(v) > 0$ such that the set $\mathcal{Z}(v_k^{\mathrm{f}})$ constructed in the proof of the previous lemma is attracting (in the τ_k^{f} direction) as long as $\dot{v}_k^{\mathrm{f}}(t) < b(v_k^{\mathrm{f}}(t))$. Moreover, as long as $v_k^{\mathrm{f}}(t)$ stays in any compact set not containing $v_\star$, we can choose a uniform $B > 0$ where $\dot{v}_k^{\mathrm{f}}(t) < B$ means the fixed point is attracting.*

Proof. This is a straightforward but tedious calculation. We compute

$$\frac{\partial}{\partial \tau_k^{\mathrm{f}}} R(t, \tau_k^{\mathrm{f}}) = c_{\mathrm{f}}(\phi(v))c_{\mathrm{f}}'(v)v' + c_{\mathrm{f}}(v)c_{\mathrm{f}}'(\phi(v))\left\{D_t\phi(v) - v' D_v\phi(v)\right\},$$

where we drop some of the dependence on the arguments for simplicity. Collecting the terms for v' gives

$$\{c_{\mathrm{f}}(\phi(v))c_{\mathrm{f}}'(v) - c_{\mathrm{f}}(v)c_{\mathrm{f}}'(\phi(v))D_v\phi(v)\}v' + c_{\mathrm{f}}(v)c_{\mathrm{f}}'(\phi(v))D_t\phi(v). \tag{32}$$

We want this quantity to be negative. By inspection, the second term in this expression is always negative, since $c_{\mathrm{f}}(v) > 0$, $D_t\phi > 0$, and c_{f} is monotone decreasing. On the other hand, one can see that the coefficient of v' is positive since it is the difference between a positive and a negative term. Thus the entire quantity (32) is negative if and only if

$$v' < \frac{-c_{\mathrm{f}}(v)c_{\mathrm{f}}'(\phi(v))D_t\phi(v)}{c_{\mathrm{f}}(\phi(v))c_{\mathrm{f}}'(v) - c_{\mathrm{f}}(v)c_{\mathrm{f}}'(\phi(v))D_v\phi(v)}, \tag{33}$$

and by inspection this is always positive. Moreover, the numerator goes to zero only if $v \to v_\star$, so on any compact set not containing $v_\star$, this fraction is uniformly bounded below. □

Proof of theorem 1. The proof has three parts. First, we will show that under these assumptions, all shocks created propagate to the right and exist for all time. Second, we show how the induction given in lemma 2 applies here and gives us the C^1-estimates. Finally, we compute how the $t_{k,i}$ grow in k.

Infinite-time existence of shocks. We see that $v_1^{\mathrm{b}}(t_1^{\mathrm{cb}}) = \phi_+^{t_+}(v_1^{\mathrm{f}}(t_1^{\mathrm{cf}}))$ and this is greater than $v_\star$ by assumption. Now, note that $v_2^{\mathrm{f}}(t_2^{\mathrm{cf}})$ must lie between $v_1^{\mathrm{f}}(t_1^{\mathrm{cf}})$ and v_n since v_n is the attracting fixed point of $\phi_v^{t_+}(\phi_-^{t_-}(\cdot))$, and in fact $v_k^{\mathrm{f}}(0) \to v_n$ monotonically as $k \to \infty$, and similarly $v_k^{\mathrm{b}}(t_k^{\mathrm{cb}}) \to v_a$ monotonically. From this it follows that $v_k^{\mathrm{f}}(t_k^{\mathrm{cf}}) < v_\star$, $v_k^{\mathrm{b}}(t_k^{\mathrm{cb}}) > v_\star$, for all k, and thus all the wavefronts and wavebacks move to the right at the time of their creation. After that, the only way for a pulse to disappear would be for a wavefront and a waveback to collide, and this can only happen if $\tau_k^{\mathrm{f}}(t)$ or $\tau_k^{\mathrm{b}}(t)$ become 0 for some t. But this is not possible, as one can see from (26), (27). For example, since $v_k^{\mathrm{f}}(t) < \alpha < v_\star$ for all t, if $\tau_k^{\mathrm{f}}(t) < v_\star - \alpha$, then

$$\phi_+^{\tau_k^{\mathrm{f}}(t)}(v_k^{\mathrm{f}}(t - \tau_k^{\mathrm{f}}(t))) < v_\star,$$

which in particular means that

$$c_{\mathrm{f}}(\phi_+^{\tau_k^{\mathrm{f}}(t)}(v_k^{\mathrm{f}}(t - \tau_k^{\mathrm{f}}(t)))) > 0.$$

For τ_k^{f} sufficiently small, $\dot{\tau}_k^{\mathrm{f}}(t) > 1$. There is no way for $\tau_k^{\mathrm{f}}(t)$ to reach 0, and thus $x_k^{\mathrm{b}}(t)$ will not collide with $x_k^{\mathrm{f}}(t)$. The argument is the same for $\tau_k^{\mathrm{b}}(t)$. Thus these shocks persist for all time.

C^1-estimates. By the assumptions of the theorem, $\phi_+^{t_+}(\phi_-^{t_-}(\cdot))$ has a unique attracting fixed point, which in particular means that $v_k^{\mathrm{f}}(t_k^{\mathrm{cf}}) \to v_n$, $v_k^{\mathrm{b}}(t_k^{\mathrm{cb}}) \to v_a$ as $k \to \infty$. So, for any δ', we can choose k_0 so that

$$|v_{k_0}^{\mathrm{f}}(t_{k_0}^{\mathrm{cf}}) - v_n| < \delta'.$$

The conclusions of the proposition hold for $k = k_0$, although in this case $t_{k_0,1}$ and $t_{k_0,3}$ might be small. Using lemma 2, we have that

$$|v_{k_0+1}^{\mathrm{f}}(t) - v_n| < C_1\delta',$$

for all $t < t_{k_0+1}^{\mathrm{cf}} + C_2$, where C_1, C_2 are defined in the statement of lemma 2. Iterating this lemma gives us that

$$|v_{k_0+k}^{\mathrm{f}}(t) - v_n| < C_1^k\delta',$$

for all $t < t_{k_0+k}^{\mathrm{cf}} + kC_2$. If we choose v_n, v_a so that $C_1 < 1$, then we can easily make this as small as we would like.

The argument is more complicated if $C_1 > 1$. What we must do is pick a $T > 0$ and show that there is a k so that the conclusion of the proposition is true, with $t_{k,1} > T$. Choose $K' > T/C_2$ and δ' with $\delta > C_1^{K'}\delta'$. There is a k_0 with $|v_{k_0}^{\mathrm{f}}(t_{k_0}^{\mathrm{cf}}) - v_n| < \delta'$, and from this

$$|v_{k_0+K'}^{\mathrm{f}}(t) - v_n| < \delta \qquad \text{for } t < T,$$

and thus $t_{k_0+K',1} \geqslant T$.

The proof for the second estimate is even easier. Clearly, if

$$|v_k^{\mathrm{f}}(t) - v_n| < \delta \qquad \text{for } t > t_{k,2},$$

then it follows from a phase-plane analysis similar to that in lemma 2 that there is a $t_{k+1,2}$ such that for all $t > t_{k+1,2}$,

$$|v_{k+1}^{\mathrm{f}}(t) - v_n| < \delta.$$

This is because once the function $v_k^{\mathrm{f}}(t)$ becomes essentially constant, it follows that $\tau_k^{\mathrm{f}}(t)$ and thus $v_k^{\mathrm{b}}(t)$ also do so, and furthermore that $v_k^{\mathrm{b}}(t)$ is very close to v_a. In a very similar fashion, we then can deduce that $v_{k+1}^{\mathrm{f}}(t)$ stays very close to v_n and in fact approaches it asymptotically.

Growth of $t_{k,i}$. To see that the time it takes to match velocities with the initial condition grows linearly in k, consider the system in the moving frame with velocity $c(v_0)$, with the variable $\xi = x - c(v_0)t$. The kth wavefront is created at the point $\xi = -c(v_0)t_k^{\mathrm{cf}}$. But its position when it is in equilibrium with v_0 is $k\xi_{eq}$, where

$$\xi_{eq} = c(v_0)(\tau_-(v_0) + \tau_+(v_0)).$$

But $t_k^{\mathrm{cf}} = k(t_- + t_+)$, and since we have chosen v_0 to not be v_n, this means that

$$t_- + t_+ \neq \tau_-(v_0) + \tau_+(v_0),$$

and thus the difference between the initial position of the kth front and its equilibrium position grows linearly in k. Since the right-hand side of (26) is uniformly bounded above, the time it takes to reach equilibrium with the initial condition also grows linearly with k. □

Remark. By assuming that $\phi_+^{t_+}(v_0) > v_\star$, we have restricted v_0 so that there is no shock which is created with a negative velocity, i.e. no shock is created moving to the left. Under the assumption that $\phi_+^{t_+} \circ \phi_-^{t_-}(\cdot)$ has a unique attracting fixed point, only a finite number of shocks can be created moving in the wrong direction. For example, say that the initial condition was chosen so that the first waveback would not propagate in the correct direction. Then the

medium would stay excited past t_1^{cb} and there would be no front created at t_2^{cf} either. But since the Poincaré map has a unique attracting fixed point, and thus $\lim_{k\to\infty} v_k^{\mathsf{f}}(t_k^{\mathsf{cf}}) \to v_n$ and $\lim_{k\to\infty} v_k^{\mathsf{b}}(t_k^{\mathsf{cb}}) \to v_a$, then for sufficiently large k, $v_k^{\mathsf{f}}(t_k^{\mathsf{cf}}) < v_\star < v_k^{\mathsf{b}}(t_k^{\mathsf{cb}})$, and all subsequent shocks will be created moving to the right.

4. Second case: non-matching times

The details of the argument in this section are quite similar to those in the previous, and we will only point out where they differ. As before, we assume that the forcing is periodic, i.e. that there are two numbers t_-, t_+ such that

$$t_k^{\mathsf{cb}} - t_k^{\mathsf{cf}} = t_+, \qquad t_{k+1}^{\mathsf{cf}} - t_k^{\mathsf{cb}} = t_-,$$

and we restrict the possible choices of t_+ and t_- so that there are v_n, $v_a \in [\hat{v}_{\min}, \hat{v}_{\max}]$ with

$$\phi_+^{t_+}(v_n) = v_a, \qquad \phi_-^{t_-}(v_a) = v_n.$$

In contrast to the last section, however, we assume here that

$$c_{\mathsf{f}}(v_n) \neq c_{\mathsf{b}}(v_a). \tag{34}$$

In this case, it is not possible to have a periodic solution where the shocks are created with the correct velocities, since the excitatory times are inconsistent with the refractory times. However, it turns out that there is a periodic solution to the front-propagation equations with the same period as the forcing. First define

$$t_\star = t_+ + t_-,$$

and then for any $v \in [\hat{v}_{\min}, v_\star]$, define

$$\tau_{\mathsf{total}}(v) = \tau_+(v) + \tau_-(\tilde{v}).$$

Clearly $\tau_{\mathsf{total}}(v_\star) = 0$ and $\tau_{\mathsf{total}}(\cdot)$ is monotone decreasing, so there is a unique $\hat{v_n}$ which solves

$$\tau_{\mathsf{total}}(\hat{v_n}) = t_\star.$$

If we further define $\hat{v_a}$ so that $c_{\mathsf{b}}(\hat{v_a}) = c_{\mathsf{f}}(\hat{v_n})$, then it is clear that

$$\tau_+(\hat{v_n}) + \tau_-(\hat{v_a}) = t_\star,$$
$$c_{\mathsf{f}}(\hat{v_n}) = c_{\mathsf{b}}(\hat{v_a}).$$

In short, $\hat{v_n}$, $\hat{v_a}$ are chosen to be the v values which give rise to a periodic wavetrain where the speed of the wavefronts matches the speed of the wavebacks, and the total period (in time) of one pulse is the same as the total period of the forcing.

The rest of this section contains the proof of the statement that the effect of the forcing in the unmatched case is such a wavetrain.

We also note here that we are guaranteed that either

$$\hat{v_n} < v_n \text{ or } \hat{v_a} > v_a,$$

namely that the periodic loop of the response in the phase plane is guaranteed to lie outside the periodic loop of figure 5. The argument for this is simply as follows: by (34) and since $c_{\mathsf{f}}(\cdot)$ and $c_{\mathsf{b}}(\cdot)$ are monotone, it follows that $\hat{v_a} \neq v_a$ and $\hat{v_n} \neq v_n$. Assume that

$$\hat{v_n} > v_n \text{ and } \hat{v_a} < v_a.$$

Then clearly the time it takes to integrate from $\hat{v_n}$ to $\hat{v_a}$ along S_+ is strictly less than t_+, and similarly the time it takes to ingrate from $\hat{v_a}$ to $\hat{v_n}$ along S_- is strictly less than t_-, and thus

$$\tau_{\mathsf{total}}(\hat{v_n}) < t_\star,$$

which is a contradiction.

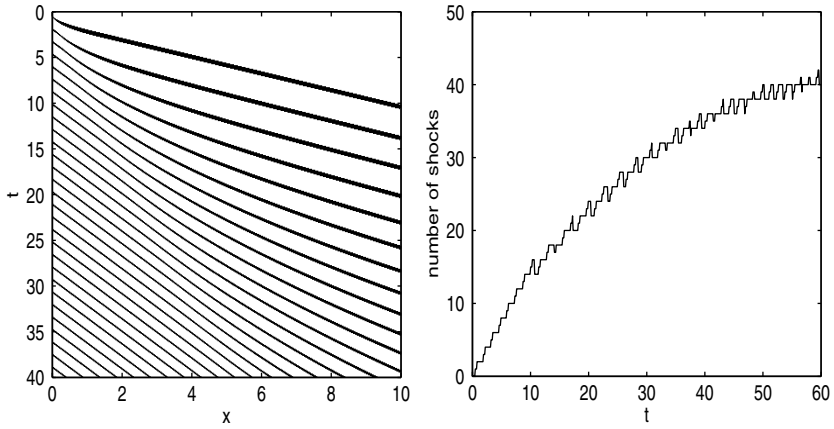

Figure 8. The left frame is as in figure 7, where we plot as black all points where $u(x, t) > 1$ and white otherwise. Here we have chosen $v_n = -0.2$ and $v_a = 0.6$. The right frame plots the number of shocks contained in the domain $x \in [0, 10]$ in the solution, versus time. This oscillates for long times because the pulses move off to the right of this domain at different times from when they are created.

As we did in the previous section, we consider first the case where the initial condition matches the forcing and then consider the general case where it does not.

Consider the solution with $v_1^{\mathrm{f}}(t) = \hat{v_n}$ and denote $c_{\mathrm{f}}(\hat{v_n}) = c_\star$. Without loss of generality, let us assume that $c_{\mathrm{b}}(v_a) > c_{\mathrm{f}}(v_n)$, i.e. in the forcing the wavebacks are being created too early and are initially moving too quickly. We move into the moving frame with velocity $c_\star$, using the coordinate $\xi = x - c_\star t$. The first wavefront is created at $\xi = 0$ and does not move. All subsequent pulses can move when they are created, but notice that each wavefront is created at its equilibrium position. On the other hand, the wavebacks are created too early, or in this picture, too far to the right. Let us denote the spatial period of the periodic solution with speed $c_\star$ by $\xi_\star$, and we can calculate that $\xi_\star = t_\star c_\star$.

First, no shock can move more than $\xi_\star$ from its initial position because it can be shown that the shocks will not crash into each other (the proof is the same as in the previous section). Fix an $\epsilon > 0$. As long as a given shock is more than ϵ away from its equilibrium position, it follows from (26), (27) that it will move, in the moving frame, with velocity greater than $C_\epsilon > 0$. Thus, it follows that every shock reaches an ϵ neighbourhood of its equilibrium position in a time which depends only on ϵ, not on k.

Similarly, if we consider the moving frame with some velocity $c \neq c_\star$, then, in this frame, the fronts are not created at their equilibrium positions. In fact, the ξ-distance from $x_k^{\mathrm{f}}(t_k^{\mathrm{cf}})$ to its equilibrium position is proportional to $(c - c_\star)k$, just as in the analogous case in the previous section. Since the velocity of these fronts is uniformly bounded above, the amount of time it takes x_k^{f} to reach its equilibrium position grows linearly in k.

In summary, it is easy to see that after some relaxation which will take place in $O(1)$ time, the solution will settle to the periodic wavetrain with the same time period as the forcing.

This also gives insight into the case where we have chosen an initial which does not match the forcing: assume for example that $v_1^{\mathrm{f}}(t) = v_0$, where $c(v_0) \neq c_\star$. Then go into the moving frame with speed $c(v_0)$. According to the preceding arguments, the kth wavefront will settle quickly to the speed $c_\star$ and then after some time (this time grows linearly in k) settles to $c(v_0)$.

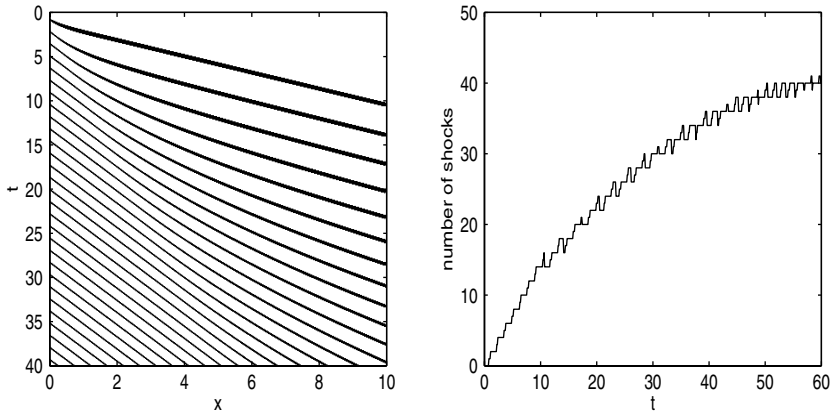

Figure 9. The left frame is as in figure 8, where we plot as black all points where $u(x, t) > 1$ and white otherwise. Here we have chosen $v_n = -0.3612$ and $v_a = 0.3612$. The right frame plots the number of shocks contained in the domain $x \in [0, 10]$ in the solution versus time. Note that these figures are almost indistinguishable from those in figure 8, as predicted by the theory of this section.

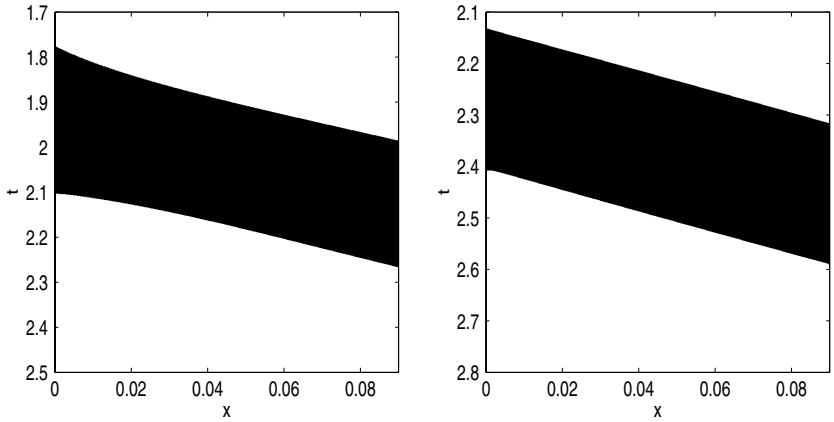

Figure 10. As in earlier figures, we are using black for all points where $u(x, t) > 1$ and white otherwise. Here we have zoomed close to the origin to see the effect of unmatched forcing: the left frame is $v_n = -0.2$, $v_a = 0.65$, whereas the right frame is $v_n = -0.35$, $v_a = 0.35$. These two have the same total period and are thus close for x far away from the origin. As we can see here empirically, the quick transient where the wavespeeds are unmatched does not survive for very long.

To see numerical examples, consider figures 8 and 9. In the first we have chosen v_n, v_a to be unmatched, in particular $v_n = -0.2$ and $v_a = 0.6$. According to the arguments in this section, to see the long-term behaviour of the solution, we need to choose $\hat{v_a}, \hat{v_n}$ so that their wavespeeds match, but they have the same total period. One can compute numerically that in this case $\hat{v_n} \approx -0.3612$, $\hat{v_a} \approx 0.3612$. We can see that the solutions in figures 8 and 9 are almost indistinguishable. The fast correction to get a pulse with consistent wavespeeds happens extremely quickly and cannot be distinguished on this graph. To see just how quickly the equilibrium is reached, consider figure 10, where one can see the the wavefronts and wavebacks move into equilibrium extremely quickly.

Acknowledgments

The authors would like to thank Cyrill Muratov for useful commentary and discussion. RELD was supported as a Courant Instructor during this work. The work of EV-E was partially supported by NSF via grant DMS02-39625 and by ONR via grant N00014-04-1-0565.

References

[1] Chen X 1992 Generation and propagation of interfaces in reaction–diffusion systems *Trans. Am. Math. Soc.* **334** 877–913
[2] Lee DeVille R E, Vanden-Eijnden E and Muratov C B 2005 Two distinct mechanisms of coherence in randomly perturbed dynamical systems *Phys. Rev.* E **72** 031105
[3] Lee DeVille R E, Muratov C B and Vanden-Eijnden E 2006 Non-meanfield deterministic limits in chemical reaction kinetics far from equilibrium *J. Chem. Phys.* **124** 231102
[4] Muratov C, Vanden-Eijnden E and Weinan E 2005 Self-induced stochastic resonance in excitable systems *Phys. D: Nonlinear Phenom.* **210** 227–40
[5] Weinan E, Ren W and Vanden-Eijnden E 2004 Minimum action method for the study of rare events *Commun. Pure Appl. Math.* **57** 637–56
[6] Faris W G and Jona-Lasinio G 1982 Large fluctuations for a nonlinear heat equation with noise *J. Phys.* A **15** 3025–55
[7] Fife P C 1976 Pattern formation in reacting and diffusing systems *J. Chem. Phys.* **64** 554–64
[8] Fitzhugh R 1960 Thresholds and plateaus in the Hodgkin–Huxley nerve equations *J. Gen. Physiol.* **43** 867–96
[9] Freidlin M I 1988 Random perturbations of reaction–diffusion equations: the quasi deterministic approximation *Trans. Am. Math. Soc.* **305** 665–97
[10] Freidlin M I 2001 On stable oscillations and equilibriums induced by small noise *J. Stat. Phys.* **103** 283–300
[11] Freidlin M I and Wentzell A D 1998 *Random Perturbations of Dynamical Systems* 2nd edn (New York: Springer)
[12] Jones C K R T 1984 Stability of the travelling wave solution of the FitzHugh–Nagumo system *Trans. Am. Math. Soc.* **286** 431–69
[13] Jung P and Mayer-Kress G 1995 Noise controlled spiral growth in excitable media *CHAOS* **5** 458–62
[14] Keener J P 1980 Waves in excitable media *SIAM J. Appl. Math.* **39** 528–48
[15] Kohn R V, Reznikoff M and Vanden-Eijnden E 2005 Magnetic elements at finite temperature and large deviation theory *J. Nonlinear Sci.* **15** 223–53
[16] Lindner B, García-Ojalvo J, Neiman A and Schimansky-Geier L 2004 Effects of noise in excitable systems *Phys. Rep.* **392** 321–424
[17] Meron E 1992 Pattern formation in excitable media *Phys. Rep.* **218** 1–66
[18] Muratov C B, Vanden-Eijnden E, Weinan E 2006 Noise can play an organizing role for the recurrent dynamics in excitable media *Proc. Natl Acad. Sci.*submitted
[19] Murray J D 2002 *Mathematical Biology. I (Interdisciplinary Applied Mathematics vol 17* 3rd edn (New York: Springer)
[20] Nii S 1997 Stability of travelling multiple-front (multiple-back) wave solutions of the FitzHugh–Nagumo equations *SIAM J. Math. Anal.* **28** 1094–112
[21] Reznikoff M 2004 Rare events in finite and infinite dimensions *PhD Thesis* New York University
[22] Rinzel J and Maginu K 1984 Kinematic analysis of wave pattern formation in excitable media *Nonequilibrium Dynamics in Chemical Systems (Bordeaux, 1984) (Springer Series in Synergetics), vol 27* (Berlin: Springer) pp 107–113
[23] Shardlow T 2004 Nucleation of waves in excitable media by noise *Multiscale Models Simul.* **3** 151–67
[24] Shardlow T 2005 Numerical simulation of stochastic PDEs for excitable media *J. Comput. Appl. Math.* **175** 429–46
[25] Soravia P and Souganidis P E 1996 Phase-field theory for Fitzhugh–Nagumo-type systems *SIAM J. Math. Anal.* **27** 1341–59
[26] Fife C P and Tyson J J 1980 Target Patterns in a realistic model of the Belousov–Zhabotinskii Reaction *J. Chem. Phys.* **73** 2224–37
[27] Tyson J J and Keener J P 1988 Singular perturbation theory of traveling waves in excitable media (a review) *Physica D* **32** 327–61